Contributions of the Hadley and Ferrel Circulations to the Energetics of the Atmosphere over the past 32-years

Contributions of the Hadley and Ferrel Circulations to the Energetics of the Atmosphere over the past 32-years

Junling Huang, School of Engineering and Applied Sciences, Harvard University, 29 Oxford Street, Cambridge, Massachusetts, 02138, USA

Corresponding author: Michael B. McElroy, School of Engineering and Applied Sciences, Harvard University, 29 Oxford Street, Cambridge, Massachusetts, 02138, USA (mbm@seas.harvard.edu)

Abstract

The Hadley system provides an example of a thermally direct circulation, the Ferrel system in contrast an example of a thermally indirect circulation. In this study, we develop an approach to investigate the key thermodynamic properties of the Hadley and Ferrel systems, quantifying them using assimilated meteorological data covering the period January 1979 to December 2010. This analysis offers a fresh perspective on the conversion of energy in the atmosphere from diabatic heating to the production of atmospheric kinetic energy. The results indicate that the thermodynamic efficiency of the Hadley system, considered as a heat engine, has been relatively constant over the 32 year period covered by the analysis, averaging 2.6 %. Over the same interval, the power generated by the Hadley regime has risen at an average rate of about 0.54 TW per year, reflecting an increase in energy input to the system consistent with the observed trend in the tropical sea surface temperatures. The Ferrel system acts as a heat pump with a coefficient of performance of 12.1, consuming kinetic energy at an approximate rate of 275 TW, exceeding the power production rate of the Hadley system by 77 TW.

1. Introduction

The Lorenz Energy Cycle (Lorenz 1955) provides an instructive approach to a quantitative investigation of the energetics of the atmosphere. The uneven spatial distribution of diabatic heating in the atmosphere results in an increase in available potential energy which is converted consequently to kinetic energy maintaining the circulation of the atmosphere against friction. Grounded on this theory, creation of kinetic energy at the expense of available potential energy can be decomposed into a contribution from the meridional overturning circulation, denoted as C_Z, and a contribution from eddies, denoted as C_E. Several groups (e.g., Krueger et al. 1965; Wiin-Nielsen 1967; Oort 1964; Oort and Peixoto 1974; Oort 1983; Li et al. 2007; Kim and Kim 2013) have sought to analyze the energetics of the atmosphere following this approach. Based on daily reports from the global radiosonde network for the 10-year period from 1963 to 1973, Oort (1983) estimated C_Z and C_E as -0.15W/m^2 and 2.0W/m^2 respectively, revealing the dominant role of C_E relative to C_Z, and concluded that the indirect Ferrel circulation consumes zonal mean kinetic energy at a rate slightly exceeding production by the Hadley circulation. The importance of C_E and C_Z in the conversion of available potential energy to kinetic energy is confirmed by recent studies based on assimilated datasets including NCEP-NCAR, NCEP-R2, ERA40 and MERRA. There are discrepancies, however, in the absolute value and the sign of C_Z (Li, et al. 2007, Kim and Kim 2013). C_Z refers to a composite of three meridional overturning components: the Hadley system in the tropics, the Ferrel system in the mid-latitudes and the Polar system at high latitudes regions. An in-depth understanding of C_Z requires an independent analysis of each component. The Lorenz Energy Cycle has limitations when it comes to defining the role of individual sources in the creation of kinetic energy: it is unable, for example, to isolate the contribution from the Hadley circulation.

68 The Hadley circulation is identified with rising of warm and moist air in the equatorial region
69 with descent of colder air in the subtropics corresponding to a thermally driven direct circulation,
70 with consequent net production of kinetic energy. Many studies (e.g., Mitas and Clement 2005,
71 2006; Frierson et al. 2007; Hu and Fu 2007; Lu et al. 2007; Previdi and Liepert 2007; Seidel and
72 Randel 2007; Seidel et al. 2008; Johanson and Fu 2009; Stachnik and Schumacher 2011; Davis
73 and Rosenlof 2012; Nguyen et al. 2013; Hu et al. 2013) have sought to analyze how the Hadley
74 system has varied under the recent warming climate. Results from these investigations indicate
75 expansion and intensification of the Hadley circulation over the past several decades. A related
76 question is whether the Hadley system has became more energetic.

77 At mid-latitudes, the circulation of the atmosphere is dominated by wave-like flows. The Ferrel
78 cells represent statistical residues which result after zonal averaging of large northward and
79 southward flows associated with the quasi-stationary atmospheric waves. The Ferrel cells are
80 identified with rising motion of relatively cold air at high latitudes, sinking of relatively warm air
81 at the lower mid-latitudes, defining a thermally indirect circulation with consequent consumption
82 of kinetic energy (Peixoto and Oort 1992).

83 Grotjahn (2003) pointed out that the Carnot Cycle concept can be used to estimate the generation
84 of kinetic energy that results from the thermodynamic changes an air parcel undergoes while
85 completing an atmospheric circuit. He estimated the power of one of the Hadley cells by plotting
86 the thermodynamic properties of air parcels on a temperature - pressure diagram. In this study,
87 we extend his approach, investigating the key thermodynamic properties of the Hadley and
88 Ferrel circulations using assimilated meteorological data from the Modern Era Retrospective-
89 analysis for Research and Applications (MERRA). The analysis allow us to differentiate
90 individual contributions of the Hadley and Ferrel systems to the C_Z process. As will be shown,

the study indicates an upward trend in the power generated by the Hadley system over the past three decades, consistent with view that this system is strengthening.

2. Data and Methodology

This investigation is based on meteorological data from the MERRA compilation covering the period January 1979 to December 2010. Wind speeds, air temperature and geopotential heights were obtained on the basis of retrospective analysis of global meteorological data using Version 5.2.0 of the GEOS-5 DAS. We use the standard monthly output available for 42 pressure levels with a horizontal resolution of 1.25 ^{o} latitude × 1.25 ^{o} longitude (Rienecker et al. 2007). The tropical sea surface temperature and ENSO index is from Goddard Institute for Space Studies (Hansen et al. 1999; Hansen et al. 2010).

Stream functions defining the zonal mean circulation were computed using the continuity equation for mass expressed in zonally averaged form:

$$\frac{\partial[\bar{v}]cos\Phi}{Rcos\Phi\partial\Phi}+\frac{\partial[\bar{\omega}]}{\partial P}=0 \qquad (1)$$

where $\left[\bar{}\right]$ defines the time and zonal average operator, v the meridional wind speed in units of $m{\cdot}s^{-1}$, ω the vertical wind speed in units of $Pa{\cdot}s^{-1}$, Φ latitude and P pressure in Pa.

The mass stream function φ is given then by:

$$[\bar{v}]=g\frac{\partial\varphi}{2\pi Rcos\Phi\partial P} \qquad (2)$$

$$[\bar{\omega}]=-g\frac{\partial\varphi}{2\pi R^{2}cos\Phi\partial\Phi} \qquad (3)$$

We calculated φ using $[\bar{v}]$, while $[\bar{\omega}]$ was computed on the basis of the assimilated meteorological data through horizontal integration of equation (2) combined with vertical integration of equation (3) beginning at the top of the atmosphere where we assumed $\varphi = 0$.

3. Thermodynamic properties of the Hadley system

a. Illustration of a direct thermal circulation

Values for January 2009 mass stream functions (10^9 kg·s^{-1}), computed on the basis of the zonal average of monthly assimilated meteorological data, are presented in Fig. 1a. Positive values are indicated by warm (red) colors with negative values denoted by cold (blue) colors. The bold black contour illustrates the direction of motion (white arrows) corresponding to the direct thermal circulation of the Hadley regime. Maximum heating in January 2009 occurs south of the equator. The air is less dense as a consequence, rising due to buoyancy, cooling in the process. Reaching the top of the convection cell, the air moves northward, cooling as it radiates more energy than it absorbs before sinking eventually in the northern sub-tropics (Marshall and Plumb 2008). The loop is completed as the air moves back across the equator at the surface.

As an example of how work is produced by completing travel around one loop of the cell, we selected the segment defined by the bold black contour in Fig. 1a, corresponding to a constant mass stream function value of 70×10^9 kg·s^{-1}. The Pressure-Volume (P-V) diagram for transit of 1 kg of air around this loop is presented in Fig. 1b. At a given pressure level, while the air parcel is experiencing ascending motion, its specific volume (illustrated by the blue line) is always greater than the specific volume (expressed by the red line) associated with the descending portion of the trajectory. The area inside the loop defines the net work performed by the air parcel as it

completes travel along the indicated loop. The net work obtained by completing one circuit of the loop is given by $\oint P\, dV_s$ where V_s defines the specific volume of the air parcel.

The net work performed by the air parcel in completing this loop is estimated at 1.90 kJ. The corresponding Pressure-ΔVolume (P-ΔV) diagram is presented in Fig. 1c in which the vertical axis indicates pressure, with the specific volume change identified on the horizontal axis (at a given pressure level, the specific volume associated the ascending motion minus the specific volume associated with descending motion). The positive sign of ΔV_s in Fig. 1c implies positive net work. Fig. 1d presents the temperature-entropy (T-S) diagram for this air parcel, illustrating the changes in temperature and specific entropy that develop over a thermodynamic cycle. The red portion of the temperature-entropy cycle is associated with the downward motion, and located quite close to the blue portion associated with the upward motion, indicating a small thermodynamic efficiency. The thermodynamic efficiency (η) of the loop is defined by:

$$\eta = \frac{\oint T dS}{\int_{absorbed\ heat} T\, dS} \qquad (4)$$

where T is temperature, S is entropy and the integral $\int_{absorbed\ heat}$ in the denominator is restricted to portions of the cycle corresponding to net positive heating (namely $T \cdot dS > 0$). The entropy term can be computed as $S = c_p \ln \theta$, where c_p is the specific heat of dry air at constant pressure and θ is potential temperature.

According to the second law of thermodynamics, $dQ = TdS$, where dQ is the net heat contributed by various sources including radiative heating (solar and infrared) and release of latent heat. Thus, the denominator in equation (4) calculates the net heat absorbed by the air parcel at higher temperature in order to do mechanical work. Water vapor in the atmosphere acts

147 as a means of storing heat which can be released later. As the air ascends, it may cool and
148 become saturated; then water vapor condenses releasing latent heat. In the case of the tropical
149 atmosphere, the heat dQ is dominated by the release of latent heat (James, 1995). For the loop
150 considered here, the thermodynamic efficiency is about 4.3 %. Only a small fraction of the heat
151 supplied to the air parcel is converted to mechanical energy.

152 b. Power of the Hadley system

153 Consider two loops with constant stream function values, one inside the other (Supporting
154 Material: Fig. S1). Assume that the total mass between loops 1 and 2 is represented by M, while
155 the average time required to complete travel through the region sandwiched between loops 1 and
156 2 is expressed by t. The mass flux, denoted by F, between loops 1 and 2 is given by the
157 difference between the mass stream function values for loops 1 and 2. The net work associated
158 with travel through one complete loop is defined by $M \cdot \oint PdV_s$, while the time required to travel
159 along the loop is given by $t = \frac{M}{F}$. Thus the power generated by motion of the air sandwiched
160 between loops 1 and 2 is specified by $F \cdot \oint PdV$.

161 For each Hadley cell, the associated power may be calculated according to:

$$Power = \int_{center\ of\ the\ cell}^{edge\ of\ the\ cell} \frac{\partial(Stream\ function\ value)}{\partial \Phi} \cdot \oint PdV \cdot d\Phi \qquad (5)$$

162 Based on the assimilated meteorological data adopted here to define conditions over the past 32
163 years, we calculated the power of the Hadley cells in each hemisphere as well as their
164 combination. The composite (32-year average) monthly results are presented in Fig. 2a-c. The
165 Hadley cell identified for the Northern Hemisphere refers to the entire cell originating in the

166 Southern Hemisphere extending across the equator to the Northern Hemisphere during northern
167 hemispheric winter. A similar definition applies to the Hadley cell in the Southern Hemisphere.
168 The Hadley cell in the Northern Hemisphere, not surprisingly, reaches its peak power of 218 TW
169 in January with a minimum of 0.5 TW in July. The counterpart in the Southern Hemisphere has a
170 peak of 204 TW in August with a minimum of 32 TW in January. Considering the power
171 associated with the combination of both Hadley cells, there are two peaks, 250 TW in January,
172 205 TW in August, and two minima, 164 TW in May, 164 TW in October. The annual mean
173 power associated with the overall Hadley system amounts to 198 TW. Reflecting differences in
174 land-sea contrast between the hemispheres, the Hadley cell in the Northern Hemisphere almost
175 disappears during northern summer. Results for the power of the circulation obtained here are
176 smaller than those reported earlier by Grotjahn (2003).

177 From Fig. 2 alone, it is unclear which of the terms in Equation (5) dominates the annual cycle of
178 Hadley cell power output. Oort and Rasmusson (1970) investigated the annual cycle of the
179 Hadley circulation based on the value of the mass stream function and data for a 5-yr period
180 obtained from a dense network of upper air stations. The seasonality of the Hadley system was
181 explored further by Dima and Wallace (2003) using NCEP-NCAR data covering the period
182 1979-2001. Defining the seasonality as the principal component of the first EOF mode of the
183 mass stream function, Dima and Wallace concluded that the seasonal variation of the circulation
184 is sinusoidal. The functional similarity between these results and the seasonal cycle in Fig. 2
185 implies that large absolute values of the mass stream function are normally associated with large
186 power output of the Hadley system and vice versa.

187 The long-term variation of the power contributed by both cells is plotted in Fig. 2d, covering the
188 period January 1979 to December 2010. The conspicuous intra-seasonal fluctuation in the black

189 line reflects the strong seasonal variation of the Hadley circulation. The red line, computed using
190 a 12-month running average, indicates the existence of an inter-annual variation combined with a
191 longer-term intensification of the circulation. Linear regression of the annual mean average data
192 indicates an increase of 0.54 TW per year in total power since 1979, as defined by the blue line.
193 The associated R^2 for the regression analysis however is 0.31, indicating considerable
194 uncertainty in the magnitude of the inferred trend.

195 c. Thermodynamic efficiency of the Hadley system

196 The thermodynamic efficiency for the Hadley cell in converting heat to work can be quantified
197 in terms of the ratio of the power generated by the cell with respect to the corresponding rate for
198 net positive absorption of heat. The rate for absorption of heat is given by:

$$absorption\ rate = \int_{center\ of\ the\ cell}^{edge\ of\ the\ cell} \frac{\partial(Stream\ function\ value)}{\partial \Phi} \cdot \int_{absorbed\ heat} T\, dS \cdot d\Phi \quad (6)$$

199 Results for the thermodynamic efficiency of the Hadley cells in each hemisphere together with
200 the overall efficiency of the entire circulation are displayed as a function of months in Fig. 3a-c.
201 The Hadley cell in the Northern Hemisphere reaches its highest efficiency of 3.3 % in December
202 with a minimum of less than 0.3 % in July. The counterpart in the Southern Hemisphere has a
203 maximum efficiency of 2.9 % in April with a minimum of 2.3 % in June. The overall efficiency
204 of the entire Hadley system is relatively constant, approximately 2.6 % for each month, with a
205 relatively small associated variation with season. The efficiency calculated for the entire Hadley
206 system is weighted towards the stronger cell; thus the 0.3 % efficiency of the NH cell during July
207 doesn't affect the overall efficiency of the Hadley system, given the fact that the SH cell is
208 exceptionally strong during this month.

Although the stream function term dominates, the thermodynamic efficiency plays an important role as well. Reanalysis datasets typically indicate higher values for the overturning stream function value in the Southern Hemisphere as compared to the Northern Hemisphere (Nguyen 2012). However, the Hadley cell in the Northern Hemisphere has a slightly greater peak power with the associated efficiency of 3.2 % as compared with the peak power of the corresponding cell in the Southern Hemisphere with an efficiency of 2.3 %, reflecting the importance of thermodynamic efficiency in determining the generation of power.

The long-term trend for the overall efficiency of the entire Hadley circulation is plotted in Fig. 3d for the period January 1979 to December 2010. The strong fluctuation in the black line reflects the seasonal variation of the circulation. The red line, computed using a 12-month running average, suggests that, at least on an annually averaged basis, the efficiency has varied little over the 30-year interval covered by the present analysis. Linear regression of the annual mean average over this period provides a regression slope of -0.0029% per year with $R^2 = 0.06$, indicating no statistically significant trend in thermodynamic efficiency.

Monthly values for the heat absorption rates for the Hadley cells in each hemisphere and for the entire Hadley circulation (an average over the entire record covered in this study) are presented in Fig. 4a-c. The long-term variation of the rate at which the heat is absorbed in driving the entire Hadley circulation is plotted in Fig. 4d for the period January 1979 to December 2010. The linear regression of the annual mean average data indicates an upward trend with an increase rate of 26.7 TW/yr with $R^2 = 0.55$, as shown by the blue line. The inter-annual variation of the heat absorption rate is associated with variation in tropical sea surface temperature between 23.6 ^{o}S ~ 23.6 ^{o}N (Fig. 5b): high tropical sea surface temperatures (SSTs) corresponds to high heat absorption rate, and vice versa. The correlation between the 12 month running average of the

heat absorption rate and the tropical sea surface temperature shown in Fig. 5b exceeds 0.6, confirming their strong connection. The ENSO signal is evident also in the heat absorption rate: specifically the warm events in 1983, 1987 and 1997, in addition to the cold events in 1985, 1996 and 1999 (Fig. 5c). The correlation between the heat absorption rate and the ENSO index shown in Fig. 5c is less, 0.32, reflecting presumably the fact that the ENSO phenomenon is more localized in the Pacific region rather than distributed over the entire domain of tropical latitudes.

4. Thermodynamic properties of the Ferrel system

a. Illustration of an indirect thermal circulation

As with Section 3, we begin this section by highlighting one specific zonal mean cell. We choose a specific segment shown in Fig. 6a, defined by the bold black contour, with a constant mass stream function value of -20×10^9 kg·s^{-1}. The P-V diagram for transit of 1 kg around this loop is presented in Fig. 6b. In contrast to the Hadley circulation, while the air parcel is experiencing ascending motion, its specific volume (illustrated by the blue line) is always smaller than the specific volume (expressed by the red line) associated with the descending portion of the trajectory. The net work consumed by the air parcel in completing this loop is estimated at 3.43 kJ. The corresponding P-ΔV diagram is presented in Fig. 6c. The T-S cycle in Fig. 6d is much rounder than that in Fig. 1d, reflecting the stronger temperature contrast at mid-latitudes, indicating the high efficiency of the Ferrel system in consumption of kinetic energy (Lorenz 1967).

The coefficient of performance (COP) of the loop is defined by:

$$\mathrm{COP} = \frac{\int_{absorbed\ heat} T\,dS}{\oint T dS} \qquad (7)$$

where the integral in the denominator is restricted to portions of the cycle corresponding to net positive heating. For the loop considered here, the COP is approximately 13.2. A parcel of air executing such a path illustrates the function of a thermodynamic heat pump. The low latitude Hadley cells act to convert thermal heat to kinetic energy: while the middle latitude Ferrel cells have the opposite effect.

b. The power consumption rate of the Ferrel system

With the same approach used to evaluate the key thermodynamic properties of the Hadley circulation, we calculated the power consumption rate, the COP and heat absorption rate of the Ferrel cells in each hemisphere as well as their combination (Fig. 7-9). The annual mean power consumption associated with the overall Ferrel system amounts to 275 TW, consistent with the conclusion reached by Oort (1983) that the Ferrel system consumes kinetic energy at a rate larger than the rate at which power is produced by the Hadley system. The overall COP of the entire Ferrel circulation is relatively constant, approximately 12.1 for each month, with a relatively small associated variation with season. If the Ferrel system were allowed to circulate in the opposite direction as a thermal engine, its efficiency would be 1 / (1+COP) = 7.6% , significantly greater than that of the Hadley system. The average rate at which heat is absorbed from the cold area by the entire Ferrel circulation over the past 32 years amounts to approximately 3.3 PW. Heat is released at the warmer area of the Ferrel system at a rate of (3.3 PW + 275 TW) = 3.6 PW.

5. Summary and Discussion

The Hadley, Ferrel and Polar circulations all contribute to the zonal mean kinetic energy budget of the atmosphere as illustrated by Fig. 10. The present study indicates an upward trend of the

power generated by the Hadley circulation over the past 32-year period. The analysis suggests that despite the apparent increase in the heat absorption rate, the thermodynamic efficiency of the Hadley circulation has remained relatively constant. Additional input of heat resulted however in a net increase in work performed and thus an increase in production of kinetic energy. The increase in the heat absorption rate over the period covered in this study amounted to 26.7 TW/year, or 0.1 W/ ($m^2 \cdot$ year) averaged over the equatorial region dominated by the Hadley circulation (30^oS to 30^oN). The positive trend in the heat absorption rate generally follows the positive trend in surface temperatures observed between 23.6 ^oS ~ 23.6 ^oN (Fig. 5b).

Regarding the energetics of a Hadley cell, we conclude that, in addition to the absolute value of the mass stream function, the thermodynamic efficiency is an important factor in determining the power output. The thermodynamic efficiency is influenced by the profiles of temperature and pressure in the atmosphere. Observational analysis have shown that the Hadley circulation has undergone statistically significant poleward expansion in the past few decades (Hu and Fu, 2007). As the Hadley circulation expanded, the temperature and pressure profiles adjusted accordingly. The present results fail to indicate any statistically significant trend in the thermodynamic efficiency.

On the intensification of the Hadley circulation, both Mitas and Clement (2005) and Hu et al. (2005) found evidence for intensification of the Hadley circulation in the NCEP/NCAR reanalysis. Since large absolute values of the mass stream function are normally associated with large power output of the Hadley system, the upward trend in the power output of the Hadley system indicated here is in general agreement with the conclusions from previous studies. Mitas and Clement (2006) pointed out that the trend might reflect systematic observational errors. Hu, Zhou, and Liu (2011) argued that the increasing trend in the Hadley circulation strength in ERA-

297 40 might be artificial as well. The MERRA data used in this study were processed in three
298 separate streams. The data distribution adopted here used Stream 1 for 1st January 1979 to 31st
299 December 1992, Stream 2 for 1st January 1993 to 31st December 2000, and Stream 3 for 1st
300 January 2001 to the present. Despite differences in the NCEP/NCAR used in the earlier studies
301 and the MERRA data employed here, conclusions in both cases are in agreement with respect to
302 the temporal intensification of the Hadley circulation.

303 The Ferrel circulation is an indirect meridional overturning circulation in mid-latitudes. The
304 rounder shape of T-S cycle in Fig. 6d as compared to Fig. 1d confirms Lorenz's 1967 expectation
305 that the stronger horizontal temperature contrast at mid-latitudes should enhance the power
306 consumption ability of the Ferrel system. The analysis implies that there has been no statistically
307 significant trend in the power consumption rate of the Ferrel circulation over the past 32-years.

308 The contribution of the Hadley and Ferrel circulations in combination have been responsible for
309 net consumption of kinetic energy at an annually averaged rate of 77 TW or 0.15W/m^2 over the
310 past 32 years (Fig. 11). The Polar meridional cell is too weak to allow its contribution to be
311 calculated following the procedure adopted here for the Hadley and Ferrel systems. The Polar
312 circulation is direct, expected therefore to contribute a net source of kinetic energy. Its
313 contribution is unlikely to significantly offset the net sink attributed here to the combination of
314 the Hadley and Ferrel systems.

315 Kim and Kim (2013) analyzed the Lorenz Energy Cycle using standard daily output of MERRA
316 dataset covering the period 1979 - 2008. Based on two different formulations, they estimated C_Z
317 to be -0.06 or -0.13W/m^2, which is in agreement with results obtained here.

Peixoto and Oort (1983) pointed out that C_E is the dominant term in the creation of kinetic energy, and simplified the conversion from available potential energy to kinetic energy process as $P_E \rightarrow K_E$, and the zonal mean kinetic energy creation process as $K_E \rightarrow K_M$ (all symbols used here are defined in the caption to Fig. 10). Thus they concluded that the energy cycle in the atmosphere proceeds from P_M to K_M through the scheme: $P_M \rightarrow P_E \rightarrow K_E \rightarrow K_M$. According to Kim and Kim (2013), C_K ($K_E \rightarrow K_M$ process) and C_E ($P_E \rightarrow K_E$ process) amount to 0.33 W/m^2 and 1.45 W/m^2 respectively, the absolute values of which are comparable to that of the power generated by the Hadley or Ferrel systems. This study provides a more comprehensive picture for P_M to K_M as summarized in Fig.10.

Acknowledgements

The work described here was supported by the National Science Foundation. Junling Huang was also supported by the Harvard Graduate Consortium on Energy and Environment. We acknowledge helpful and constructive comments from Brian F. Farrell, Zhiming Kuang, Michael J. Aziz, and Xi Lu. We are indebted also to two anonymous referees for helpful suggestions.

References

Davis, S. M., and K.H. Rosenlof, 2012: A multidiagnostic intercomparison of tropical-width time series using reanalyses and satellite observations. *J. Climate*, **25**, 1061-1078.

Dima, I. M., and J.M. Wallace, 2003: On the seasonality of the Hadley cell. *J. Atmos. Sci.*, **60**, 1522–1527.

Frierson, D. M. W., J. Lu, and G. Chen, 2007: Width of the Hadley cell in simple and comprehensive general circulation models. *Geophys. Res. Lett.*, **34**, L18804

Grotjahn, R., 2003: Energy Cycle. *Encyclopedia of Atmos. Sci.*, 829–841

Hansen, J., R. Ruedy, J. Glascoe, and M. Sato, 1999: GISS analysis of surface temperature change. *J. Geophys. Res.*, **104**, 30997-31022.

Hansen, J., R. Ruedy, M. Sato, and K. Lo, 2010: Global surface temperature change. *Rev. Geophys.*, **48**, RG4004

Hu, Y., K.K. Tung, and J. Liu, 2005: A closer comparison of early and late-winter atmospheric trends in the northern hemisphere. *J. Climate*, **18**, 3204-3216.

Hu, Y., and Q. Fu, 2007: Observed poleward expansion of the Hadley circulation since 1979, *Atmos. Chem. Phys.*, **7**, 5229–5236.

Hu, Y., C. Zhou, and J. Liu, 2011: Observational evidence for poleward expansion of the Hadley circulation. *Adv. Atmos. Sci.*, **28**, 33-44.

Hu, Y., L. Tao, and J. Liu, 2013: Poleward expansion of the Hadley circulation in CMIP5 simulations. *Adv. Atmos. Sci.*, **30**, 790-795.

James, I. N., 1995: *Introduction to circulating atmospheres*. Cambridge University Press, 74 pp.

Johanson, C. M., and Q. Fu, 2009: Hadley cell widening: Model simulations versus observations. *J. Climate*, **22**, 2713–2725.

Kim, Y. H., and M. K. Kim, 2013: Examination of the global lorenz energy cycle using MERRA and NCEP-reanalysis 2. *Climate Dynamics*, 1-15.

Krueger, A. F., J. S. Winston, and D. A. Haines, 1965: Computation of atmospheric energy and its transformation for the Northern Hemisphere for a recent five-year period. *Mon. Wea. Rev.*, **93**, 227– 238.

Li, L., A. P. Ingersoll, X. Jiang, D. Feldman, and Y. L. Yung, 2007: Lorenz energy cycle of the global atmosphere based on reanalysis datasets. *Geophys. Res. Lett.*, **34**, L16813.

Lorenz, E. N., 1955: Available potential energy and the maintenance of the general circulation. *Tellus*, **7**, 157-167.

----------, 1967: *The natural and theory of the general circulation of the atmosphere*. World Meteorological Organization, 109 pp.

Lu, J., G.A. Vecchi and T. Reichler, 2007: Expansion of the Hadley cell under global warming. *Geophys. Res. Lett.*, **34**, L06805.

Marshall, J., and R. A. Plumb, 2008: *Atmosphere, ocean, and climate dynamics: an introductory text*. Academic Press, 74 pp.

Mitas, C. M., and A. Clement, 2005: Has the Hadley cell been strengthening in recent decades? *Geophys. Res. Lett.*, **32**, L03809.

Mitas, C. M., and A. Clement, 2006: Recent behavior of the Hadley cell and tropical thermodynamics in climate models and reanalyses. *Geophys. Res. Lett.*, **33**, L01810.

Nguyen, H., A. Evans, C. Lucas, I. Smith, and B. Timbal, 2013: The Hadley Circulation in Reanalyses: Climatology, Variability, and Change. *J. Climate*, **26**, 3357-3376.

Oort, A. H., 1964: On estimates of the atmospheric energy cycle. *Mon. Wea. Rev.*, **92**, 483-493.

----------, 1983: Global atmospheric circulation statistics, 1958– 1973 (No. 14). NOAA, U.S. Gov. Print. Off., 180 - 226.

Oort, A. H., and E. M. Rasmusson, 1970: On the annual variation of the monthly mean meridional circulation. *Mon. Wea. Rev.*, **98**, 423-442.

Oort, A. H., and J. P. Peixóto, 1974: The annual cycle of the energetics of the atmosphere on a planetary scale. J. Geophys. Res., **79**, 2705-2719.

Peixoto, J. P., and A. H. Oort, 1992: *Physics of Climate*. AIP Press, 160 pp.

Previdi, M., and B. G. Liepert, 2007: Annular modes and Hadley cell expansion under global warming. *Geophys. Res. Lett.*, **34**, L22701.

Rienecker, M. et al., 2007: The GEOS-5 data assimilation system—Documentation of versions 5.0.1 and 5.1.0. NASA GSFC, Tech. Rep. Series on Global Modeling and Data Assimilation, NASA/TM-2007-104606, Vol. 27.

Seidel, D. J., and W. J. Randel, 2007: Recent widening of the tropical belt: Evidence from tropopause observations. *J. Geophys. Res.*, **112**, D20113.

414 Seidel, D. J., Q. Fu, W. J. Randel, and T. J. Reichler, 2008: Widening of the tropical belt in a
415 changing climate. *Nature Geosci.*, **1**, 21–24.

416 Stachnik, J. P., and C. Schumacher, 2011: A comparison of the Hadley circulation in modern
417 reanalyses. *J. Geophys. Res.*, **116**, D22102.

418 Wiin-Nielsen, A., 1967: On the annual variation and spectral distribution of atmospheric energy.
419 *Tellus*, **19**, 540–559.

420

421

422

423

424

425

426

427

428

429

430

431

Figures

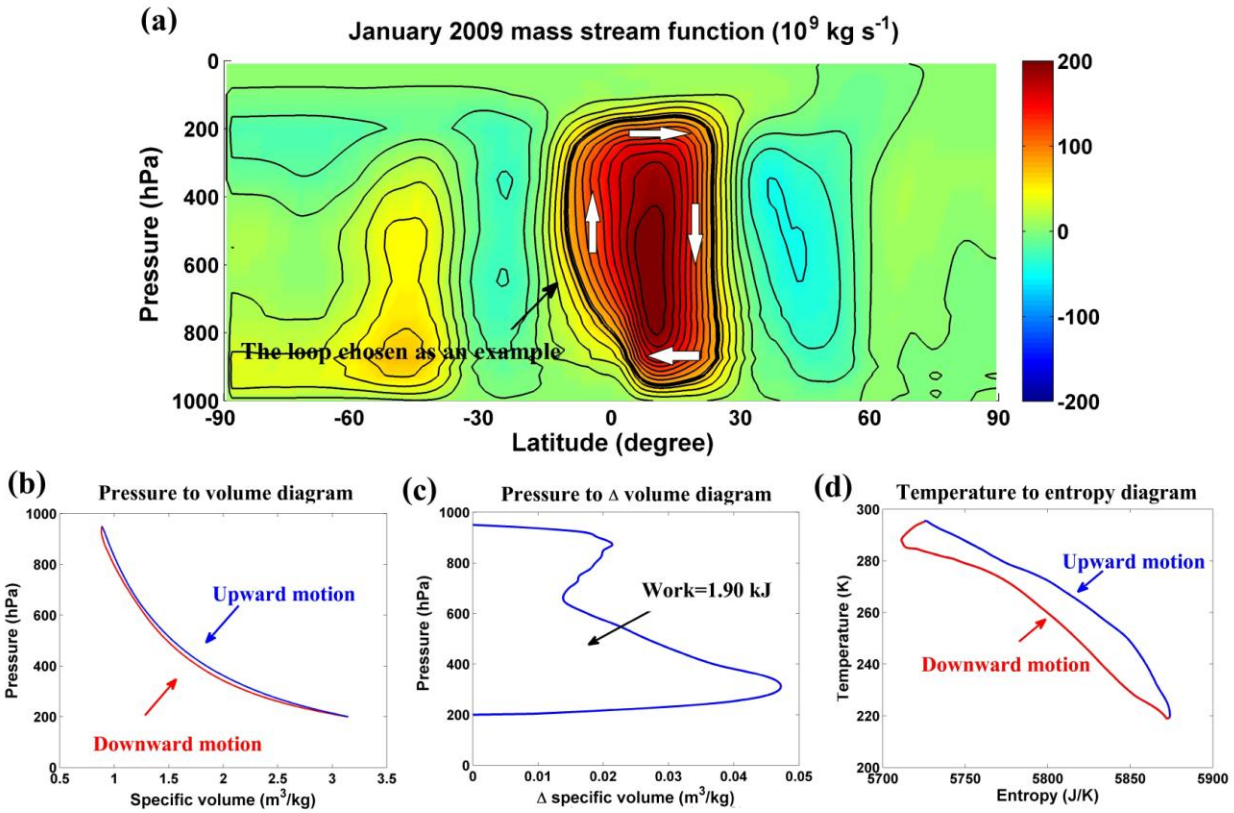

FIG. 1. The average meridional circulation of the atmosphere in January 2009 with emphasis on the direct Hadley system. Colors in panel (a) specify mass stream function values in units of 10^9 kg s^{-1}. The bold black loop, with constant mass stream-function value of 70×10^9 kg·s^{-1}, is chosen as an example to illustrate the thermally driven direct circulation. White arrows point in the direction of air motion. Panel (b) displays the P-V diagram for an air parcel with mass stream-function value of 70×10^9 kg·s^{-1}. Panel (c) presents the P-ΔV diagram for an air parcel with mass stream-function value of 70×10^9 kg·s^{-1}. Panel (d) illustrates the T-S diagram for an air parcel with mass stream-function value of 70×10^9 kg·s^{-1}.

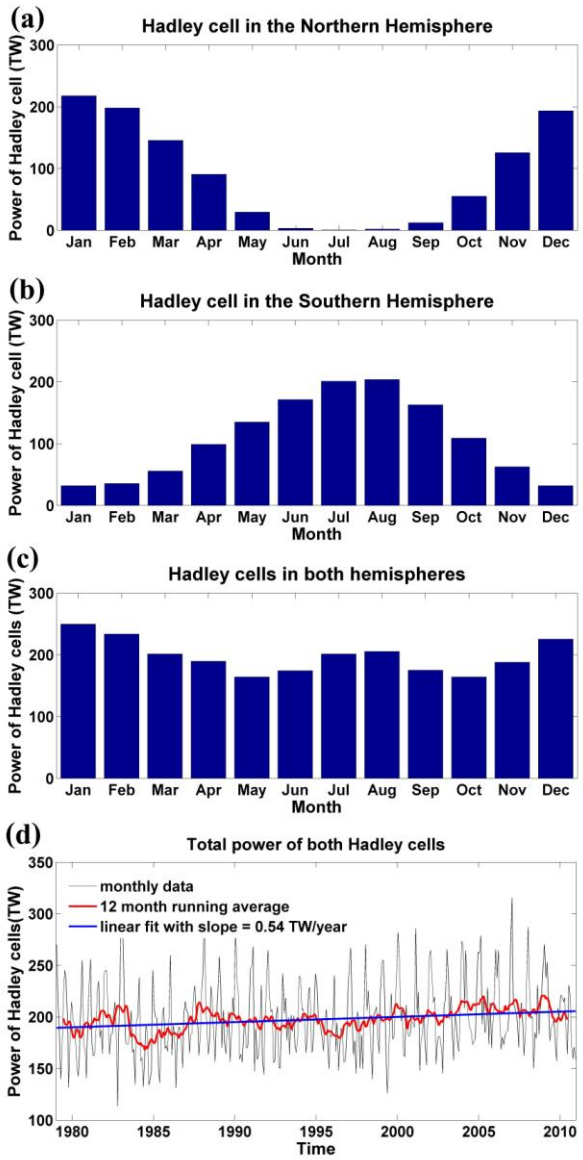

442

443 FIG. 2. The power of the Hadley circulation: (a) The power of the Hadley cell in the Northern
444 Hemisphere as a function of month; (b) The power of the Hadley cell in the Southern
445 Hemisphere as a function of month; (c) The total power of both Hadley cells as a function of
446 month; (d) The variation of the total power of both Hadley cells from January 1979 to December
447 2010.

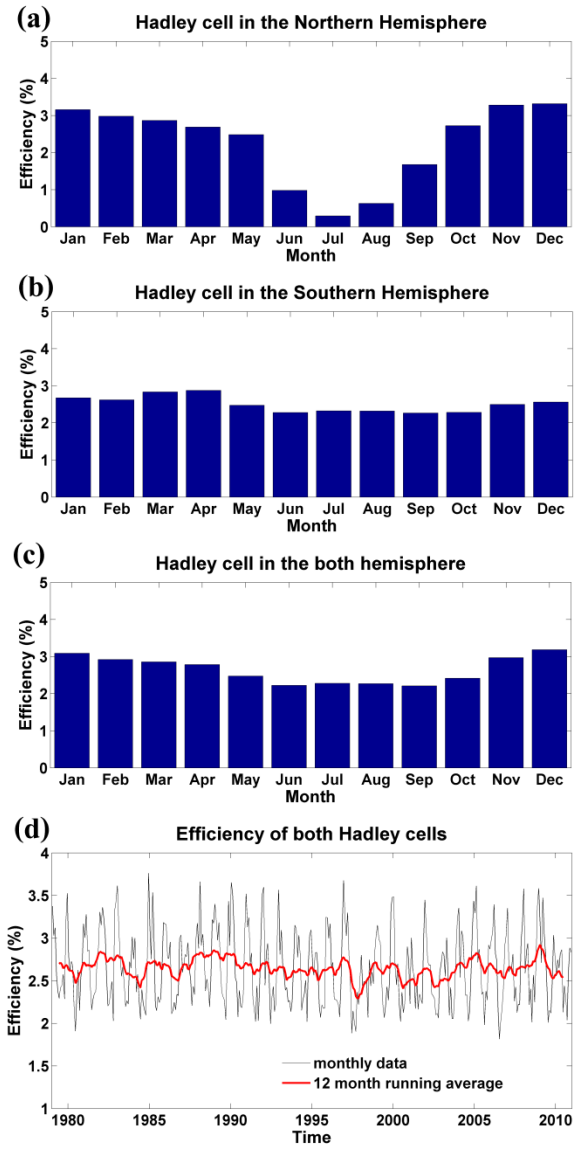

448

449 FIG. 3. The efficiency of the Hadley circulation: (a) The efficiency of the Hadley cell in the
450 Northern Hemisphere as a function of month; (b) The efficiency of the Hadley cell in the
451 Southern Hemisphere as a function of month; (c) The overall efficiency of both Hadley cells as a
452 function of month; (d) The variation of the overall efficiency of both Hadley cells from January
453 1979 to December 2010.

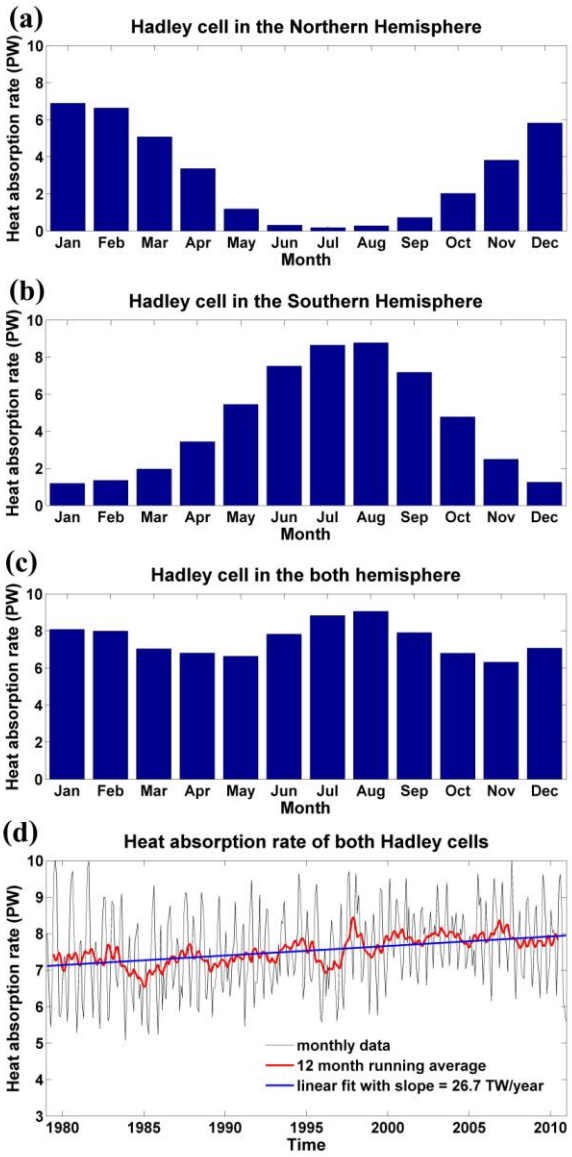

454

455 FIG. 4. The heat absorption rate of the Hadley circulation: (a) The heat absorption rate of the
456 Hadley cell in the Northern Hemisphere as a function of month; (b) The heat absorption rate of
457 the Hadley cell in the Southern Hemisphere as a function of month; (c) The overall heat
458 absorption rate for both Hadley cells as a function of month; (d) The variation of the total heat
459 absorption rate for both Hadley cells from January 1979 to December 2010.

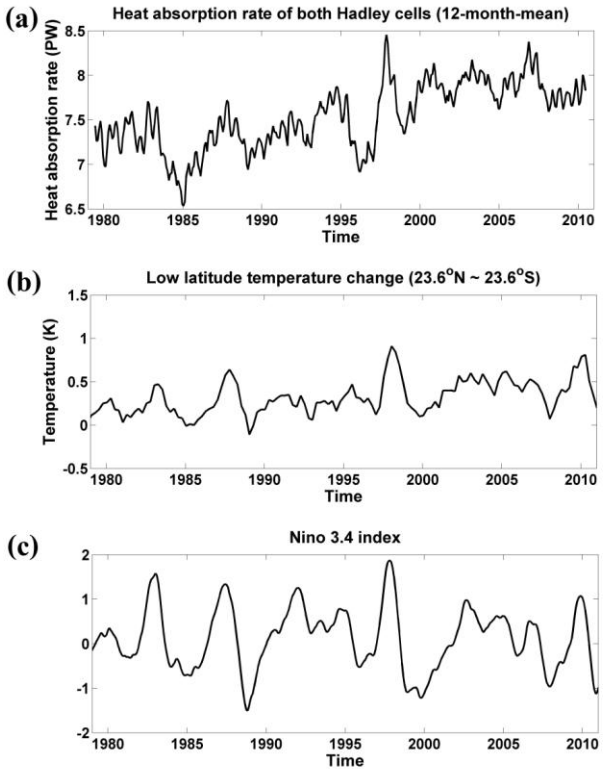

460

461 FIG. 5. Variations of heat absorption rates of both Hadley cells, low latitude temperatures and
462 the Enso index: (a) 12-month running average of the total heat absorption rate for both Hadley
463 cells from January 1979 to December 2010; (b) Changes in mean tropical temperature (data
464 available at: http://data.giss.nasa.gov/gistemp) over the period January 1979 to December 2010;
465 (c) Nino 3.4 index (data available at: http://www.esrl.noaa.gov/psd/data/climateindices) over the
466 period January 1979 to December 2010.

467

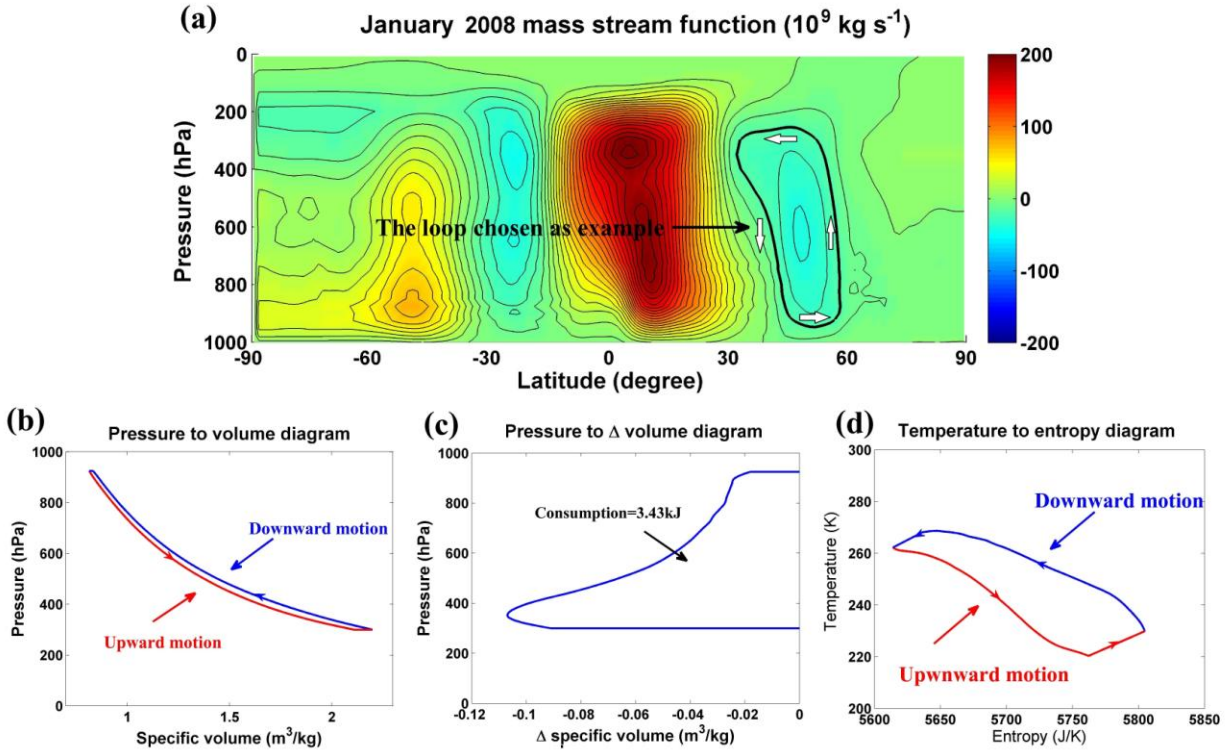

468

469 FIG. 6. The average meridional overturning of the atmosphere in January 2008 with emphasis on
470 the indirect Ferrel circulation. Colors in panel (a) specify mass stream function values in units of
471 10^9 kg·s^{-1}. The bold black loop, with constant mass stream-function value of -20×10^9 kg·s^{-1}, is
472 chosen as an example to illustrate the thermally driven direct circulation. White arrows point in
473 the direction of air motion. Panel (b) presents the P-V diagram for an air parcel with mass
474 stream-function value of -20×10^9 kg·s^{-1}. Panel (c) displays the P-ΔV diagram for an air parcel
475 with mass stream-function value of -20×10^9 kg·s^{-1}. Panel (d) illustrates the T-S diagram for an air
476 parcel with mass stream-function value of -20×10^9 kg·s^{-1}.

477

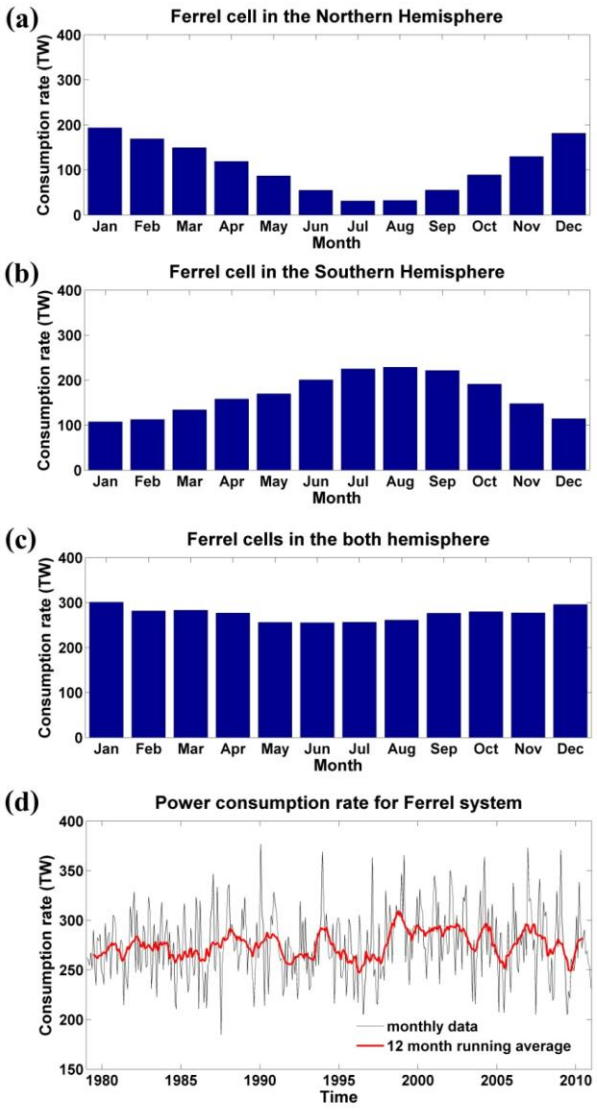

478

479 FIG. 7. The power consumption rate of the Ferrel circulation: (a) The power consumption rate of
480 the Ferrel cell in the Northern Hemisphere as a function of month; (b) The power consumption
481 rate of the Ferrel cell in the Southern Hemisphere as a function of month; (c) The total power
482 consumption rate of both Ferrel cells as a function of month; (d) The variation of the total power
483 consumption rate of both Ferrel cells from January 1979 to December 2010.

484

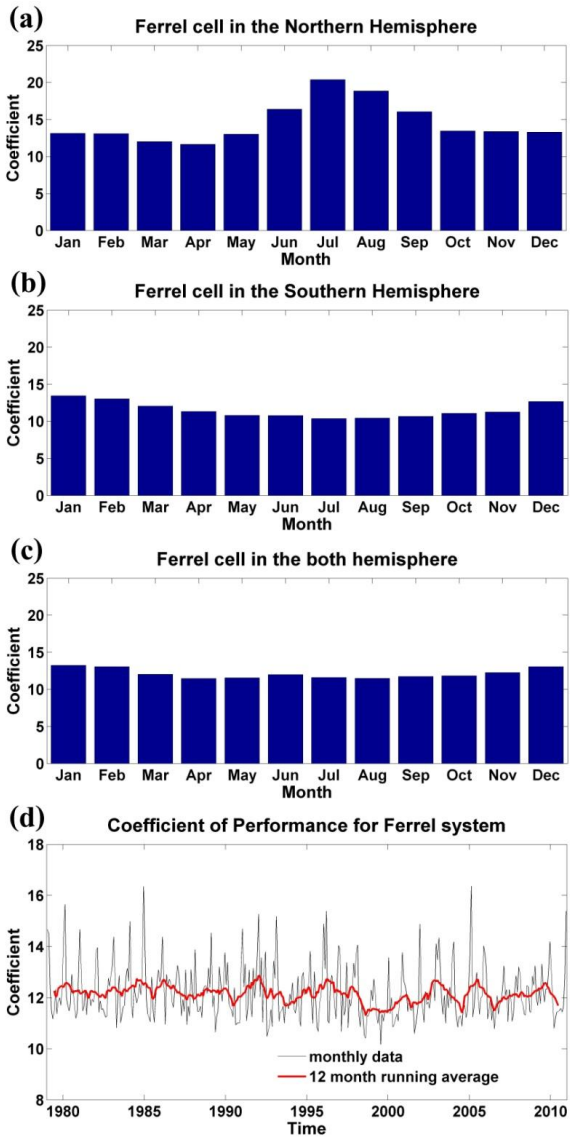

485

486 FIG. 8. The COP of the Ferrel circulation: (a) The COP of the Ferrel cell in the Northern
487 Hemisphere as a function of month; (b) The COP of the Ferrel cell in the Southern Hemisphere
488 as a function of month; (c) The overall COP of both Ferrel cells as a function of month; (d) The
489 variation of the overall COP of both Ferrel cells from January 1979 to December 2010.

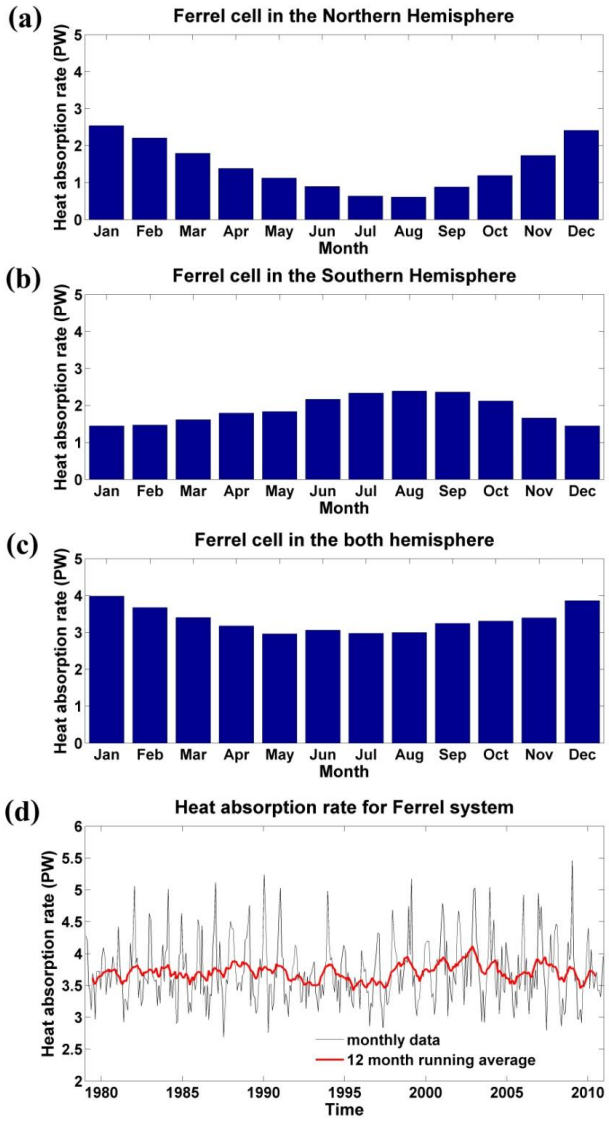

490

491 FIG. 9. The heat absorption rate of the Ferrel circulation: (a) The heat absorption rate of the
492 Ferrel cell in the Northern Hemisphere as a function of month; (b) The heat absorption rate of the
493 Ferrel cell in the Southern Hemisphere as a function of month; (c) The overall heat absorption
494 rate for both Ferrel cells as a function of month; (d) The variation of the total heat absorption rate
495 of both Ferrel cells from January 1979 to December 2010.

496

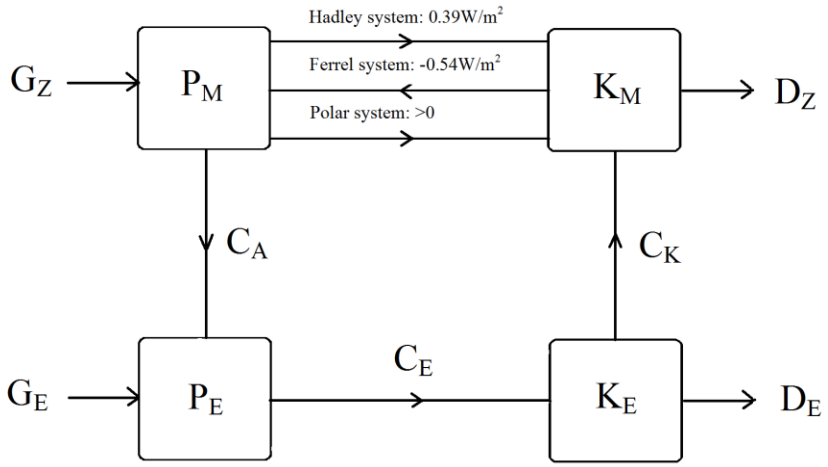

FIG. 10. Lorenz Energy Cycle with decomposition of the kinetic energy source C_Z. P_M is the mean available potential energy; P_E the eddy available potential energy; K_M the mean kinetic energy; K_E the eddy kinetic energy; G_z the creation of P_M; G_E the creation of P_E; C_A the conversion from P_M to P_E; C_E the conversion from P_E to K_E; C_K the conversion from K_E to K_M; D_z the dissipation of K_M and D_E the dissipation of K_E.

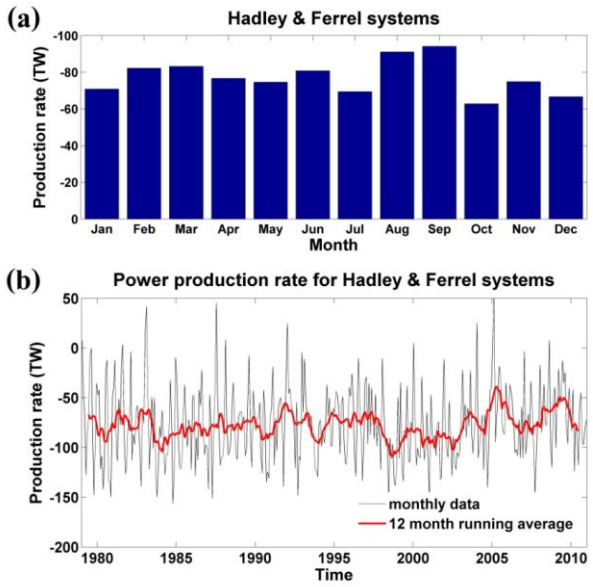

508

509 FIG. 11. The power generated by the combination of Hadley and Ferrel circulations: (a) The
510 power generated by the combination of Hadley and Ferrel circulations as a function of month; (b)
511 The power generated by the combination of Hadley and Ferrel circulations from January 1979 to
512 December 2010.